frontiers | Frontiers in Earth Science

ORIGINAL RESEARCH
published: 01 July 2022
doi: 10.3389/feart.2022.931834

Analysis of the Diagenetic Fluid of Deep Dolomitic "Leopard-Spot" Limestones in the Middle Permian Qixia Formation in Shuangyushi Region in Northwest Sichuan Basin, China

Shengyang Xie[1,2], Xingzhi Wang[1,2], Bo Li[3], Hang Jiang[4], Yao Du[5], Rui Zhang[4], Yong Li[4], Mingyang Wei[1,2], Dong Huang[1,2], Jiahao Kang[1,2], Benjian Zhang[4] and Fei Huo[1,2]**

[1]State Key Laboratory of Oil and Gas Reservoir Geology and Exploitation, Southwest Petroleum University, Chengdu, China, [2]School of Geoscience and Technology, Southwest Petroleum University, Chengdu, China, [3]Shale Gas Research Institute of PetroChina Southwest Oil & Gasfield Company, Chengdu, China, [4]Exploration Division of PetroChina Southwest Oil & Gasfield Company, Chengdu, China, [5]Exploration and Development Research Institute, PetroChina Southwest Oil & Gasfield Company, Chengdu, China

OPEN ACCESS

Edited by:
Chen Zhang,
Chengdu University of Technology, China

Reviewed by:
Tao Hu,
China University of Petroleum, China
Wenrui Shi,
Yangtze University, China
Fujie Jiang,
China University of Petroleum, China

***Correspondence:**
Shengyang Xie
xsy_time@163.com
Fei Huo
huofei342099206@163.com

Specialty section:
This article was submitted to Structural Geology and Tectonics, a section of the journal Frontiers in Earth Science

Received: 29 April 2022
Accepted: 12 May 2022
Published: 01 July 2022

Citation:
Xie S, Wang X, Li B, Jiang H, Du Y, Zhang R, Li Y, Wei M, Huang D, Kang J, Zhang B and Huo F (2022) Analysis of the Diagenetic Fluid of Deep Dolomitic "Leopard-Spot" Limestones in the Middle Permian Qixia Formation in Shuangyushi Region in Northwest Sichuan Basin, China. Front. Earth Sci. 10:931834. doi: 10.3389/feart.2022.931834

A thorough investigation of the characteristics and formation mechanism of dolomite is greatly significant in assessing the validity of dolomitization theory and dolomite reservoirs. Extensive development of dolomites has been found in the organic bank of the Middle Permian Qixia Formation in the northwest of the Sichuan Basin. For that reason, field profile and drilling core samples were collected from the common dolomitic "leopard-spot" limestones in the Middle Permian Qixia Formation in the study area and observed in this work. The diagenetic fluid and formation factors of dolomites were analyzed through major elements, microelements, carbon, oxygen and strontium (Sr) isotope, and fluid inclusion, as well as order degree of dolomite. From the extracted outcomes, valuable insights can be derived. More specifically, in the study area, dolomitic "leopard-spot" limestones were mainly developed in the upper part of Section II in the Qixia Formation. Interestingly, the vertical distribution plays a dominant role since it was transited gradually and gently to the thick-layered lumpy crystalline dolomites downward. The dolomitic "leopard-spots" are mainly composed of dolosiltite-fine crystalline dolomites with residual fabrics, and the base limestones were mainly formed by biomicrites (debris). In addition, the average $\delta^{13}C$ of dolomitic "leopard-spot" and base limestones was 3.06‰ and 3.31‰, respectively, whereas their average $\delta^{18}O$ was −4.29‰ and −3.16‰ and the $^{87}Sr/^{86}Sr$ (0.70734 in average) was higher than those of the contemporaneous seawater and mantle provenance range. Moreover, the contents of the major elements in dolomitic "leopard-spot" and base limestones were basically consistent. The uniform temperature of inclusion ranges between 70°C and 115°C. According to the geochemical data and the previously reported studies on the regional paleogeotemperature environment, the diagenetic fluid of the dolomitic "leopard-spot" limestones in the Qixia Formation in the northwest Sichuan Basin was mainly attributed to contemporaneous sea flows. However, influenced by the

local high-temperature environment, the terrestrial atmosphere, and the fresh water, it is speculated that the dolomitic "leopard-spot" limestones in the study area might belong to dolomitization involving fresh water from the penecontemporaneous stage to the early shallow burial stage.

Keywords: dolomitic "leopard-spot" limestone, dolomitization, diagenetic fluid, sedimentary environment, Sichuan Basin

1 INTRODUCTION

Dolomite is highly appreciated by petroleum geologists worldwide as an important reservoir rock, and the formation of dolomite remains an open question for the scientific community (Machel and Mountjoy, 1986; Budd, 1997; Wang et al., 2001; Warren, 2000; Zhao et al., 2018). The exploration of the dolomite reservoir in the Middle Permian Qixia Formation in Sichuan Basin, China, started in the 1970s. Several different interpretations of the formation of crystalline dolomite and dolomitic "leopard-spot" limestones in the Qixia Formation in the northwest of the Sichuan Basin have been proposed in the literature over the past 40 years. However, no consensus has been reached yet (Zhang, 1982; Song, 1985; He and Feng, 1996; Jiang et al., 2009; Huang et al., 2012; Huang et al., 2014; Tian et al., 2014; Bo et al., 2020; Li et al., 2020; Lu et al., 2020). Currently, the formation of dolomitic "leopard-spots" in the study area is maily interpreted from the perspective of the mantle hydrothermal solution. However, except for some crystalline dolomites formed by the mantle hydrothermal solution in the secondary pores in local areas (Huang et al., 2012; Chen et al., 2013; Huang et al., 2014; Han et al., 2016; Zhao et al., 2018; Hu et al., 2019), no fractures for the longitudinal or lateral migration of mantle the hydrothermal solution in the study area were found. Therefore, there was no prerequisite for the formation of large-scale dolomitic "leopard-spot" limestones and large-scale stratigraphic crystalline dolomites. In fact, dolomites in the study area are significantly influenced by atmospheric fresh water and high temperature (Bo et al., 2020; Li et al., 2020). In other words, freshwater intervention and the fast rise of the formation temperature in the depositional stage of the Qixia Formation are regarded as the two major factors that decisively affect the large-scale dolomitic "leopard-spot" limestones. Additionally, several dolomitization modes have been summarized and established in the literature in previous associated studies to explain the formation of dolomites (Badiozamani, 1973; Bathurst, 1975; Friedman, 1980; Longman, 1980; Sibley, 1991; Tucker, 1991; Vasconcelos et al., 1995; Mazzullo, 2009). However, there is no completely definite theoretical mode that could interpret the underlying formation mechanism of dolomite in the whole study area. Therefore, the diagenetic fluid of "leopard-spot" dolomite in the study area was thoroughly discussed by combining tectonics, sedimentary facies, macroscopic and microscopic features of the minerals, and the geochemical test in the region. The acquired results can provide references to study dolomitization and the dolomite reservoir in the Qixia Formation in the study area in the future.

2 GEOLOGICAL SETTING

The study area was located in the Shuangyushi Tectonic belt in the northwest of Sichuan Basin, covering Guangyuan City, Jiange County, and Qingchuan County (**Figure 1A**). It is in front of the Longmen Mountain and bordered by mountains in the back. Middle-deep cutting middle-height mountain landform exists, and the overall terrain is high in the northwest but low in the southeast. Low mountains and hills are dominant in the southeast, whereas middle-deep cutting middle-height mountains are in the northwest region, where steep mountains and narrow valleys can be found (Wang et al., 2016; Yuan et al., 2010). In tectonics, the study area is located in the secondary tectonic unit on the border between the ancient middle-depression lower belt in the northern Sichuan and the Longmenshan fold belt (**Figure 1B**), which belongs to the secondary positive tectonic units of the Zhongba-Shuangyushi higher belt. Influenced by a strong extension of the Early Emei Taphrogeny in the Hualixi Movement during Permian, an Emeishan large igneous province was formed in the Western Sichuan Province due to abundant basaltic magma erupts. The study area is located in the northeast region of this Emeishan large igneous province, where a relatively stable tectonic environment exists. Moreover, some highland regions are formed in the study area in the great background of the Hercynian Uplift, which has a relatively surface temperature and manifested as a shallow-water carbonate platform environment (Zhang et al., 2011; Yang et al., 2014) (**Figure 1C**).

The Permian Qixia Formation is in conformable contact with the overlying Maokou Formation, but it is in parallel unconformity with the underlying Liangshan Formation (Hu et al., 2010). In the Qixia Formation, it is manifested as a set of relatively complete carbonate sedimentations controlled by the transgression-regression cycles, and its internal structure can be divided into Qiyi Section and Qier Section from the bottom up, which are in conformable contact (Guoqi et al., 2010; Luo et al., 2017; Bo et al., 2020). In the study area, the Middle Permian shallow-water carbonate platform is the dominant environment, in which a good water cycle, normal ~ relatively high salinity, and rich biotypes can be found. In the study area, Qixia Formation is mainly composed of light gray-dark gray thin-middle stratigraphic micritic bioclastic limestone, thick bulk sparry bioclastic limestone, dolomitic "leopard-spot" limestones, and crystalline dolomite. It contains a dark thin-layered bioclastic calcareous mudstone intercalation. The shale content decreases gradually from the bottom up, and eyeball structures, chert belt, and chert nodule can be observed. Moreover, it is rich in biological fossils, mainly Fusulinida, peduncle, and acanthosis.

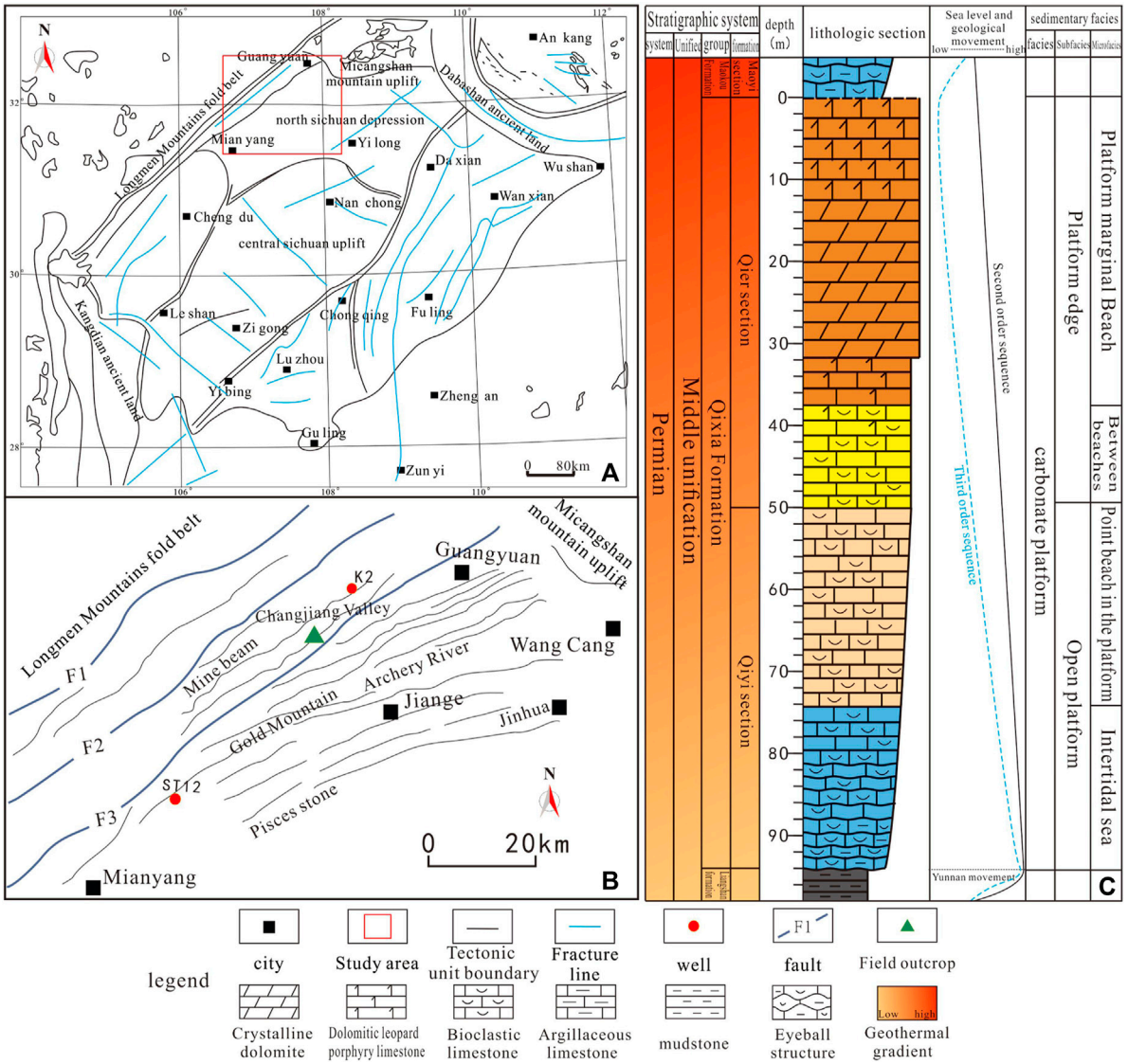

FIGURE 1 | Geology and lithology histogram of the study area.

The dolomites are mainly developed from the middle to the top of the Qier Section, and they are located in the ancient landform uplift (**Figure 1**).

3 SAMPLES AND METHODS

In this work, the Changjianggou Profile in Qingchuan, Guangyuan city, Sichuan province, was chosen as the field profile. Wells ST12 and K2 in the Shuangyushi Tectonics, Mianyang city, Sichuan province, were chosen as the drilling lithologic profiles. Firstly, outcrops of the Qixia Formation were observed systematically. Along these lines, more than 100 samples of the key layers were collected from top to bottom. Among them, 44 rock samples were screened for the key analysis (dolomitic "leopard-spot" limestone, bioclastic limestone, and crystalline dolomite). Later, the rock sheets were prepared in the pit according to the analysis projects, and the relevant analyses and tests were completed. All rock sheets were dyed with alizarin red solution, and the casting sheets were filled with blue epoxy resin. The sheet identification and fluid inclusion were analyzed in the Sichuan Key Laboratory of Natural Gas Geology using the Olympus BX53 microscope, the THMSG 600 cooling-heating bench, and the Leica DM2500P fluorescence microscope. During the process of the microelement test, the samples were ground into powder, filtered by a 200-mesh sieve, and melted by lithium borate. Subsequently, a quantitative analysis of plasma mass spectrometry was carried out. The isotope value was expressed in ‰ (PDB standard), and the error was smaller than ±0.1‰. The carbon and oxygen isotope samples precipitate the formation of CO_2 by the employment of a strong phosphoric acid at 72°C. The Thermo-Finnigan GasBench system was connected with the

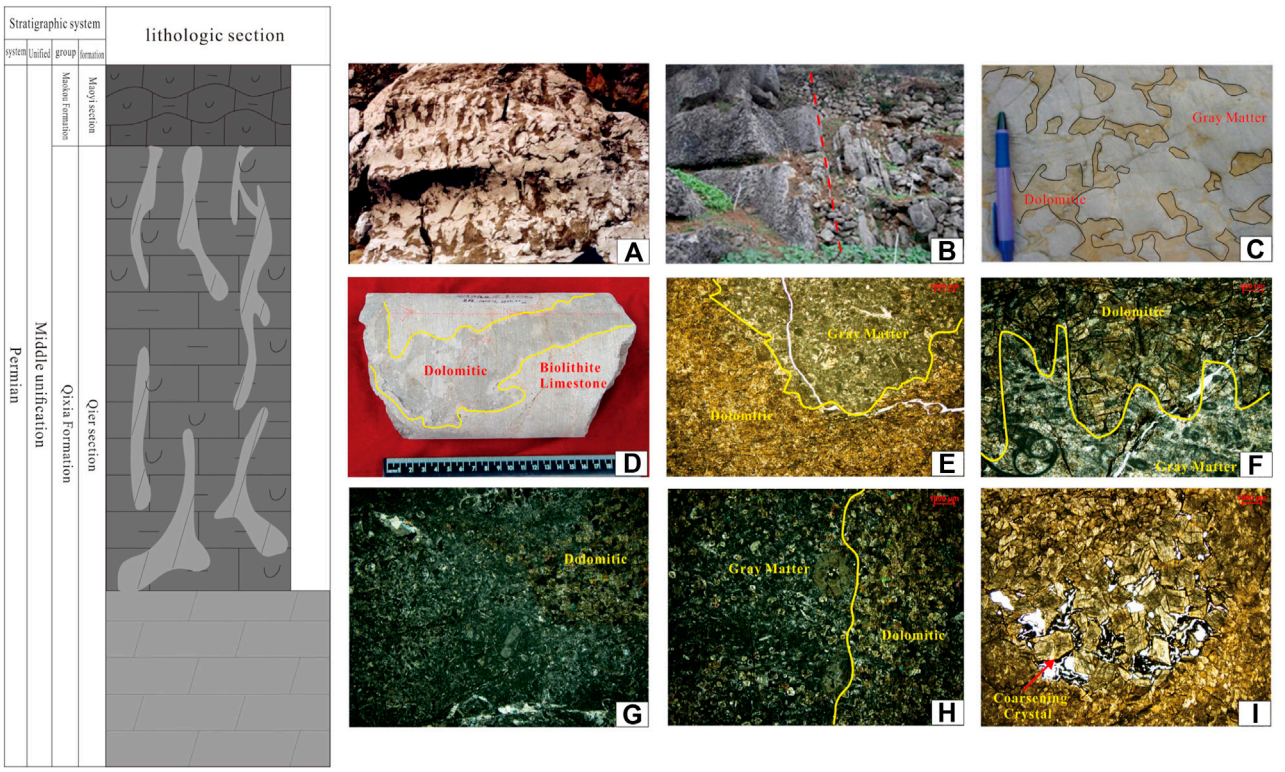

FIGURE 2 | Dolomite characteristics of Qixia Formation in the study area. **(A)** Depiction of the dolomitic "leopard-spot" limestones. Dolomization occurs due to cracking exposure, downward penetration of atmospheric fresh water along dry cracks, and mixture with seawater. As a result, base limestones have brecciated-vein structures after metasomatism. They are developed at the top of the Qixia Formation, Changyuanjiang, Guangyuan city, Sichuan province. **(B)** The thick-layered massive dolomitic "leopard-spot" limestones at the top of the Qixia Formation are in abrupt contact with the middle-thin layered "eyeball" limestones in the overlying Maoyi Section. Dolomitic "leopard-spots" are distributed approximately vertical, Jinzi Mountain, Guangyuan city. **(C)** Dolomitic "leopard-spot" limestones. Networked dry cracks are developed on the surface, indicating sedimentation discontinuity caused by a short-term outcrop. Subsequently, different corrosions are formed on the outcrop surface due to atmospheric leaching, top Qixia Formation, Changjianggou, Guangyuan city. **(D)** Dolomitic "leopard-spot" limestones, K2 well, 2405.12–2405.32 m, Qier Section. **(E)** Crystalline dolomite, development of needle-like pores and holes, ST12 well, 7077.50–7077.73 m, the upper part of Qier Section, ×10 (–). **(F)** Dolomitic "leopard-spot" limestones; dolomites are subhedral-automorphic fine-middle crystals, ST12 well, 7050.04 m, upper part of the Qier Section, ×10 (+). **(G)** Bioclastic limestone, containing red alga, foraminifer and other organisms, weak dolomitization, ST12 well, 7051.49 m, the upper part of the Qier Section, ×10 (+). **(H)** Depiction of dolomitic "leopard-spot" limestones, where dolomites are subhedral-automorphic fine-middle crystals. Limestones contain biological fossils such as crinoids, ST12 well, 7051.7 m, the upper part of the Qier Section, ×10 (+). **(I)** Crystalline dolomite, the intergranular pores are developed and the corrosion is enlarged. The contact relation of crystals is irregular. Crystal coarsening can be seen. The intergranular pores are developed, which are semi-filled by asphalt. ST12 well, 7059.9 m, Qier Section, ×10 (-).

MAT DeltaPlus isotope mass spectrometer (CF-IRMS) for the analysis. The Strontium (Sr) isotope analysis and test were completed in the Guangzhou Aoshi Analysis and Test Laboratory.

4 LITHOLOGIC FEATURES

Dolomitic "leopard-spot" limestones were extensively developed in the northwest regions of Sichuan province. The dolomitic "leopard-spot" limestones in the Qixia Formation of the study area mainly form complete sets with the underlying crystalline dolomites. They mainly exist at the top of the Qier Section in the field and downhole profiles and gradually migrate to the crystalline dolomite downward (**Figure 2**). A long-distance tracking comparison can be made within a certain range, and the formation thickness ranges between 1 and 5 m. The rock association is generally manifested as the upper dolomitic "leopard-spot" limestones, which leads to the formation of an abrupt contact with calcilutites and "eyeball-eyeball-like" limestones in the overlying Maokou Formation, which are gradually shifted to thick-layered massive crystalline dolomites. Such association may possess several cycles longitudinally. In the study area, two cycles were detected. The dolomitic "leopard-spot" limestone is a transition type between limestone and dolomite. The base limestones were composed of light-gray, gray, and dark gray bioclastic limestones, which are common in the Permian System in Sichuan Basin. Light-beige, beige, and brown crystalline dolomites are the major components of dolomitic "leopard-spots." In the dolomitic "leopard-spot" limestones, the base limestone content was generally higher than that of dolomitic "leopard-spots" (**Figures 2A,B**).

4.1 Dolomitic "Leopard-Spot" Limestones and Crystalline Dolomite

On the lithologic level of the field outcrop and drilling core, dry cracks at the top of the dolomitic "leopard-spot" limestones can be found. The exposure dry "gravels," which are often light-grey bioclastic limestones, become round due to corrosion and spaces among gravels that are filled with beige dolomitic "leopard-spots" (**Figures 2C,D**). In the longitudinal direction, dolomitic "leopard-spots" are mainly in the vertical or approximately vertical distributions at the upper parts. As it goes deeper, the emergence of dolomitic "leopard-spots" becomes flattered, accompanied by an increasing quantity and expanding area in both irregular and flocculent distribution. The proportion of the dolomitic "leopard-spots" in the base limestone increases gradually, and they are gradually shifted into the underlying thick-layered crystalline dolomite (**Figure 2A**). The underlying crystalline dolomites usually manifest as grey-white-brown grey bulks with uniform colors. Needle-like pores and holes are also developed, filled with dolomite grains and asphaltene (**Figure 2E**).

From a microscopic point of view, dolomitic "leopard-spots" are formed by irregular and uneven dolomitization of the base limestone, and they are mainly composed of anhedral ~ subhedral powder-fine crystalline dolomites. The dolomite surfaces are dirt, and dolomites look like nearly mosaic grains, with metasomatic dolomized biological and calcareous breccia residues on local areas. Some intergranular holes, intergranular dissolution pores, and small karst caves also exist, showing some reservoir accumulation (**Figures 2F–H**). The dolomite surfaces in the massive crystalline dolomites are dirt, and the grain size generally ranges from middle to coarse. Euhedral-anhedral crystals were also observed. There are primary intergranular pores in dolomites, which are expanded by erosion to some extent. The pores are filled with asphaltene and distributed along the grain edges (**Figure 2I**).

4.2 Base Limestone (Bioclastic Limestone)

Base limestones are mainly composed of thick-layered massive micritic bioclastic limestone. The mud sparry calcite is an ingredient. More specifically, the bioclastic content is higher than 50%. Red alga, green alga, foraminifer, and acanthosis limestones are the most common components. Combined with the field outcrops and identification under a microscope, most of these bioclastics are broken, but foraminifer and odonate limestones are relatively complete. Moderate-poor crystals were also chosen and rounded. The filling content in intergranular spaces is smaller than 50%, in which plaster is the major component, and a small content of sparry micrite can also be detected. The influence of the local plaster after recrystallization is changed to powder-fine crystals (**Figures 2F–H**). Some intergranular pores, inter-base micropores, and biological cavity holes were detected in the base limestones. However, most primary pores disappeared in the follow-up compaction, agglutination, and recrystallization (**Figures 2E,F**).

5 GEOCHEMICAL CHARACTERISTICS

5.1 Isotope Characteristics

C, O, and Sr isotopes have an irreplaceable impact on analyzing fluid properties and diagenetic temperature during the carbonate diagenesis process (Wang et al., 2011; Guo et al., 2003; Wang and Bai, 1999). The carbonate diagenetic fluid source can be reflected by the branch changes of the Sr isotope (Huang et al., 2002; Yan et al., 2005). In the study area, the $\delta^{13}C$ values of dolomitic "leopard-spots," base limestones, and crystalline dolomites in the Qixia Formation of the study area were 1.66‰–4.32‰ (3.06‰ on average), 2.46‰–3.96‰ (3.31‰ on average), and 1.80‰–2.82‰ (2.34‰ on average). Additionally, the $\delta^{18}O$ values were −5.87‰–1.99‰ (−4.29‰ on average), −2.27‰–4.43‰ (−3.16‰ on average), and −5.88‰–4.43‰ (−5.14‰ on average), whereas the $^{87}Sr/^{86}Sr$ values were 0.70724–0.70960 (0.70785 on average), 0.70791–0.70958 (0.707344 on average), and 0.70791–0.70958 (0.70868 on average), respectively (**Table 1**). The C and O isotope distributions are relatively similar between the dolomitic "leopard-spots" and the base limestones, indicating that the diagenetic fluid has homologous characteristics. However, the C and O isotope test values of the dolomitic "leopard-spots" and the base limestones differ significantly from those of the crystallize dolomites, indicating the manifestation of significant differences in the diagenetic fluids of dolomitic "leopard-spots," base limestones, and crystalline dolomites (**Figure 3A**). The $^{87}Sr/^{86}Sr$ values of the dolomitic "leopard-spots," base limestones, and crystalline dolomites are all higher than the variation range (0.70726–0.70742) of the $^{87}Sr/^{86}Sr$ contemporaneous seawater base limestones. This effect reveals that the diagenetic fluid of dolomitic "leopard-spots" retains most seawater ingredients (**Figure 3B**) (Xu et al., 2022).

5.2 Microelement Characteristics

In the study area, the microelement contents in dolomitic "leopard-spots," base limestones, and crystalline dolomite are significantly different (**Table 2** and **Figure 4**). According to the experimental analysis, the K, Na, Sr, and Ba elements in the base limestones are mainly distributed in the low-value regions. Interestingly, the Na content in the dolomitic "leopard-spots" is higher than that in the bioclastic limestone, and the K content has two obvious zones. Moreover, the Sr content is significantly lower, and the Ba content is obviously higher. This effect reveals that diagenetic fluid involves exogenous fluids. Compared with the crystalline dolomites, the contents of K, Na, Ba, and Sr in dolomitic "leopard-spots" are slightly higher, showing a similar composition of their diagenetic fluids.

The selected chondrite standardization analyses of the microelements such as Rb, Ba, Th, U, Nb, La, Ce, Sr, Nd, P, Zr, Hf, Sm, Y, Yb, and Lu are shown in **Table 2** and **Figure 5**. Clearly, the microelements in dolomites and limestones are relatively concentrated. In particular, microelement distributions are basically consistent between the dolomitic "leopard-spots" and the base limestones. Moreover, the microelement distribution range of the crystalline dolomite is

TABLE 1 | C and O isotope data of carbonates in Qixia Formation of ST12 in the study area.

Number of samples	Depth (m)	Lithology	$\delta^{13}C$(PDB)	$\delta^{18}O$(PDB)	Number of samples	Depth (m)	Lithology	$\delta^{13}C$(PDB)	$\delta^{18}O$(PDB)
QX8	7050.34	Dolomitic leopard-spot	3.60	−2.97	QX36	7073.2	Dolomitic leopard-spot	3.19	−4.17
QX5	7051.03	Bioclastic limestone	3.63	−3.75	QX37	7074.63	Dolomitic leopard-spot	2.32	−4.30
QX5-1	7051.03	Dolomitic leopard-spot	2.56	−3.98	QX52	7077.8	Bioclastic limestone	2.28	−5.49
QX10	7052.97	Dolomitic leopard-spot	3.92	−3.46	QX53	7077.8	Bioclastic limestone	1.99	−5.40
QX11	7052.97	Bioclastic limestone	3.33	−4.14	QX54	7078	Bioclastic limestone	2.29	−2.10
QX2	7053.63	Bioclastic limestone	3.44	−3.27	QX55	7078.96	Bioclastic limestone	1.33	−5.20
QX16	7054.4	Dolomitic leopard-spot	3.64	−3.55	QX56	7078.96	Bioclastic limestone	2.44	−5.49
QX17	7054.4	Bioclastic limestone	2.85	−4.14	QX42	7080.35	Bioclastic limestone	2.48	−5.11
QX162	7054.4	Dolomitic leopard-spot	3.97	−2.68	QX57	7083.11	Bioclastic limestone	2.08	−4.43
QX14	7056.05	Dolomitic leopard-spot	3.84	−3.94	QX58	7083.11	Bioclastic limestone	2.31	−4.91
QX15	7056.05	Bioclastic limestone	2.80	−4.43	QX44	7083.5	Bioclastic limestone	1.98	−5.88
QX18	7057.25	Dolomitic leopard-spot	3.25	−4.91	QX59	7086.2	Bioclastic limestone	2.30	−4.72
QX19	7057.25	Bioclastic limestone	2.46	−5.98	QX60	7086.55	Bioclastic limestone	2.16	−4.82
QX20	7058	Crystalline dolomite	2.35	−5.11	QX61	7086.8	Bioclastic limestone	3.52	−5.20
QX24	7061.83	Crystalline dolomite	2.75	−5.49	QX62	7088	Bioclastic limestone	2.43	−5.20
QX25	7062.85	Dolomitic leopard-spot	1.65	−5.30	QX63	7088.25	Bioclastic limestone	2.63	−5.30
QX26	7062.85	Bioclastic limestone	3.88	−2.27	QX65	7088.41	Bioclastic limestone	2.60	−4.62
QX27-1	7063.40	Dolomitic leopard-spot	4.14	−1.99	QX66	7088.41	Bioclastic limestone	2.63	−4.43
QX30	7067	Dolomitic leopard-spot	1.86	−5.43	QX67	7088.62	Bioclastic limestone	1.80	−5.49
QX31	7067	Bioclastic limestone	3.44	−3.27	QX62	7088.8	Bioclastic limestone	2.82	−4.72
QX32-1	7068.22	Bioclastic limestone	3.96	−2.67	QX46	7090.34	Bioclastic limestone	2.44	−5.59
QX34	7070	Dolomitic leopard-spot	1.92	−5.87	QX35	7071.25	Bioclastic limestone	2.14	−5.40

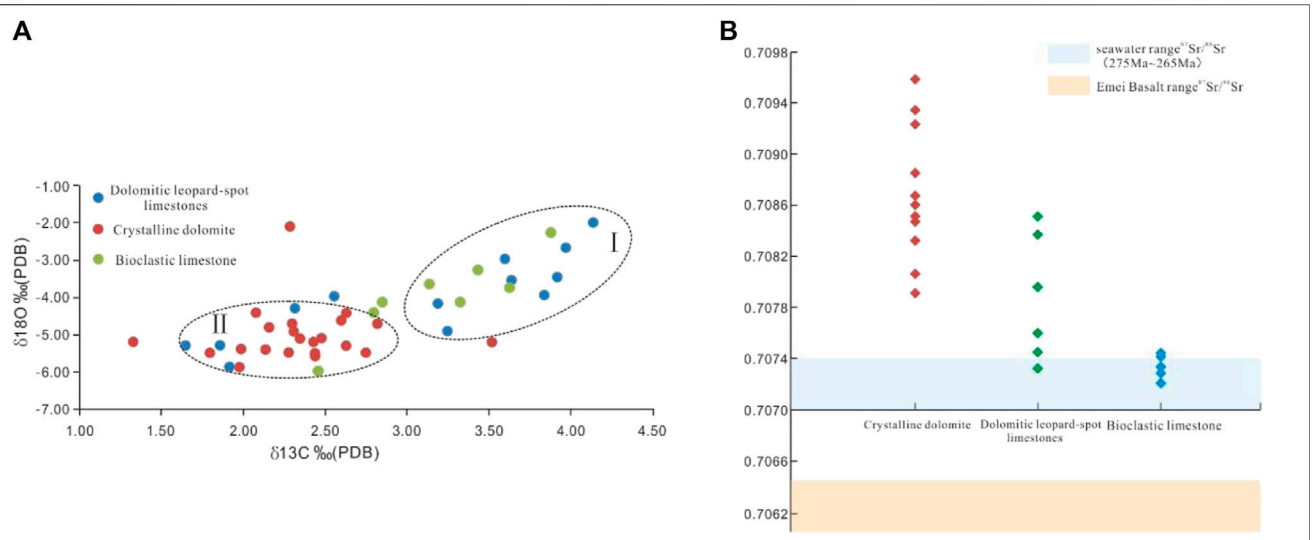

FIGURE 3 | C, O, and Sr isotope characteristics of carbonates in the Qixia Formation in the study area. **(A)** C and O isotope distribution patterns of carbonates in the Qixia Formation; I-crystalline dolomite clustering; II-dolomitic "leopard-spot" and base limestone clustering. **(B)** Sr isotope distribution of carbonate in the Qixia Formation.

relatively small, and the Th content in some crystalline dolomite is increased.

5.3 Order Degree

Order degree of dolomites is related to the crystallization velocity. The dolomites formed in the early stage have a low-order degree. With the increase in the buried depth, the order degree climbs up gradually. However, implementing a high temperature can overcome the dynamic barrier in the dolomitization process, thus resulting in lattice distortion and fast crystallization of dolomites (Zheng and Qin, 2020). The order degree of the dolomitic "leopard-spot" limestones is 0.4–0.56, which is significantly lower than that of the crystalline dolomite (0.48–0.68) (**Table 3**).

5.4 Fluid Inclusion Characteristics

Fluid inclusion refers to the diagenetic fluid, which is wrapped during mineral crystallization in the diagenesis process. In minerals, fluid inclusion exhibits an obvious boundary with

TABLE 2 | Carbonate microelement test results of Qixia Formation in the study area (chondrite standardization).

Number of samples	Lithology	K	Na	Sr	Ba	Rb*	Ba*	Th*	U*	Nb*	La*	Ce*	Sr*	Nd*	P*	Zr*	Hf*	Sm*	Y*	Yb*	Lu*
		%	%	μg/g	μg/g	Chondrite standardization; Boynton (1984)															
QX3	Dolomitic leopard-spot	0.04	0.04	109.5	39.8	0.69	16.51	8.28	25.00	0.81	2.58	1.86	15.08	1.00	0.02	0.23	0.93	0.67	1.40	0.57	0.60
QX4	Bioclastic limestone	0.03	0.03	113.0	18.1	0.52	7.51	6.90	21.25	0.81	2.58	1.61	15.56	1.00	0.01	0.21	0.93	0.92	1.27	0.57	0.60
QX63	Crystalline dolomite	0.01	0.03	55.0	6.3	0.13	2.61	1.38	21.25	0.41	1.94	1.24	7.58	1.00	0.02	0.21	0.93	0.67	0.96	0.53	0.60
QX70	Crystalline dolomite	0.03	0.02	69.8	4.4	0.43	1.83	15.17	147.50	0.81	2.26	1.61	9.61	1.17	0.01	0.54	0.93	0.72	1.21	0.62	0.60
QX52	Dolomitic leopard-spot	0.01	0.03	92.2	4.9	0.17	2.03	2.07	18.75	0.41	1.94	1.11	12.70	0.83	0.06	0.13	0.93	0.77	0.76	0.33	0.30
QX58	Crystalline dolomite	0.01	0.03	72.1	21.8	0.22	9.05	3.79	31.25	0.41	2.90	2.10	9.93	1.33	0.05	0.21	0.93	0.97	1.08	0.38	0.30
QX69	Crystalline dolomite	0.01	0.02	11.6	3.3	0.04	1.37	0.69	6.25	0.41	1.61	1.24	1.60	0.83	0.01	0.13	0.93	0.56	1.02	0.33	0.30
QX47	Dolomitic leopard-spot	0.03	0.04	109.5	16.6	0.47	6.89	3.45	28.75	0.81	1.29	0.87	15.08	0.50	0.02	0.23	0.93	0.31	0.38	0.29	0.30
QX53	Dolomitic leopard-spot	0.09	0.05	126.0	19.1	1.55	7.93	15.86	32.50	2.03	4.19	2.60	17.36	1.67	0.07	1.03	0.93	0.92	1.08	0.53	0.60
QX56	Dolomitic leopard-spot	0.03	0.03	165.0	27.1	0.39	11.24	4.14	30.00	1.22	6.13	2.97	22.73	2.67	0.04	0.78	0.93	1.54	1.53	0.91	0.90
QX66	Crystalline dolomite	0.02	0.04	105.0	7.6	0.30	3.15	5.17	20.00	0.81	4.52	2.48	14.46	2.00	0.07	0.21	0.93	1.28	1.40	0.62	0.60
QX42	Crystalline dolomite	0.02	0.03	66.9	23.0	0.30	9.54	4.48	38.75	0.81	3.87	2.23	9.21	1.83	0.07	0.44	0.93	1.08	1.40	0.62	0.60
QX57	Crystalline dolomite	0.01	0.03	90.2	62.5	0.34	25.93	4.48	51.25	0.81	3.55	3.47	12.42	1.67	0.02	0.21	0.93	1.03	1.02	0.53	0.60
QX77	Dolomitic leopard-spot	0.09	0.02	117.0	5.6	1.29	2.32	12.07	132.50	2.44	3.55	2.35	16.12	1.33	0.01	1.03	0.93	0.97	0.96	0.57	0.60
QX76	Bioclastic limestone	0.02	0.01	208.0	2.8	0.34	1.16	7.93	38.75	0.41	2.90	2.10	28.65	1.17	0.01	0.26	0.93	0.67	0.64	0.33	0.30
QX54	Crystalline dolomite	0.15	0.04	148.5	32.7	1.77	13.57	22.41	378.75	10.57	10.00	5.82	20.45	6.00	0.25	4.39	3.74	4.15	2.74	1.53	1.51
QX62	Crystalline dolomite	0.33	0.05	130.5	32.1	3.71	13.32	45.86	276.25	26.02	10.32	7.05	17.98	4.83	0.20	12.92	11.21	3.49	2.17	1.24	1.20
QX65	Crystalline dolomite	0.03	0.04	140.0	57.5	0.39	23.86	4.83	18.75	0.41	8.06	3.96	19.28	4.00	0.06	0.16	0.93	2.05	1.85	0.91	0.90
QX67	Crystalline dolomite	0.63	0.06	99.7	58.8	6.72	24.40	61.72	65.00	37.40	17.10	9.03	13.73	6.17	0.28	17.31	14.02	4.36	2.61	1.20	0.90
QX44	Crystalline dolomite	0.70	0.05	116.5	68.1	6.72	28.26	57.59	652.50	36.18	20.97	12.62	16.05	11.17	0.71	16.28	14.95	7.49	3.89	1.67	1.51
QX55	Dolomitic leopard-spot	0.43	0.06	134.0	30.5	3.79	12.66	38.97	402.50	25.20	10.00	5.82	18.46	4.33	0.22	11.37	11.21	2.82	2.04	0.91	0.90
QX48	Bioclastic limestone	0.02	0.03	131.0	3.0	0.30	1.24	2.76	28.75	0.41	0.97	0.74	18.04	0.50	0.02	0.18	0.93	0.26	0.19	0.14	0.30
QX50	Bioclastic limestone	0.01	0.02	103.5	3.0	0.13	1.24	1.38	16.25	0.41	1.29	0.74	14.26	0.50	0.02	0.13	0.93	0.41	0.51	0.14	0.30
QX51	Bioclastic limestone	0.01	0.02	130.5	2.8	0.13	1.16	1.03	17.50	0.41	1.29	0.74	17.98	0.50	0.02	0.13	0.93	0.26	0.45	0.24	0.30
QX61	Crystalline dolomite	0.01	0.03	56.6	78.6	0.13	32.61	2.41	16.25	0.41	0.97	0.62	7.80	0.50	0.02	0.13	0.93	0.31	0.25	0.24	0.30
QX68	Crystalline dolomite	0.01	0.03	80.3	93.6	0.09	38.84	1.03	41.25	0.41	0.97	0.62	11.06	0.33	0.02	0.16	0.93	0.26	0.38	0.14	0.30
QX71	Crystalline dolomite	0.01	0.03	46.6	2.3	0.09	0.95	2.76	111.25	0.41	0.97	0.62	6.42	0.33	0.01	0.13	0.93	0.26	0.45	0.14	0.30
QX72	Crystalline dolomite	0.01	0.02	69.7	2.3	0.09	0.95	2.07	63.75	0.41	1.61	0.87	9.60	0.50	0.01	0.13	0.93	0.46	0.64	0.24	0.30

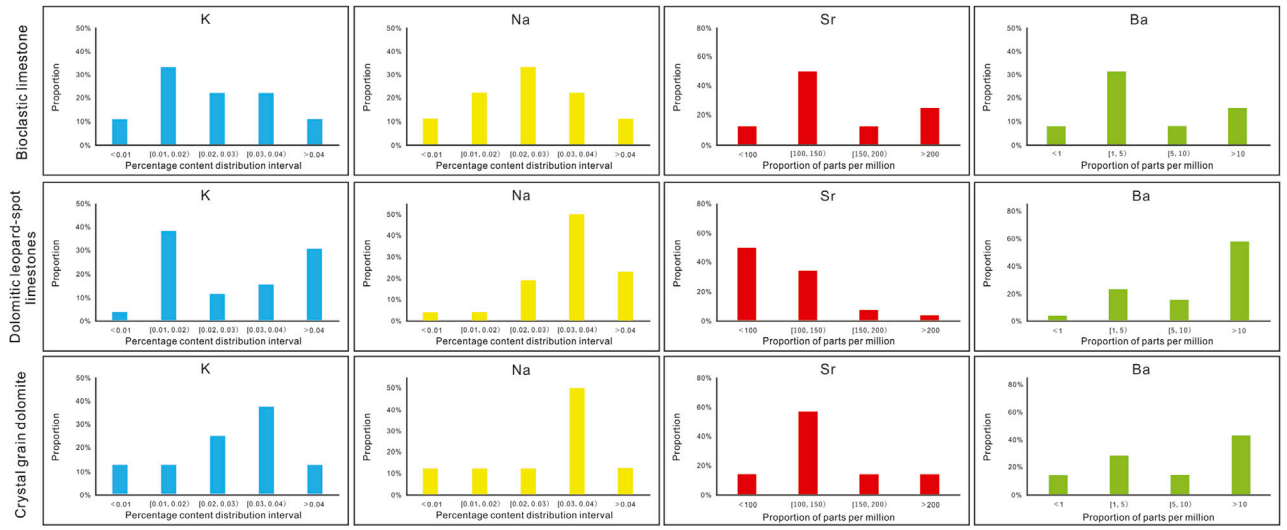

FIGURE 4 | Statistical charts of the contents of K, Na, Sr, and Ba in dolomites of the Qixia Formation in the study area.

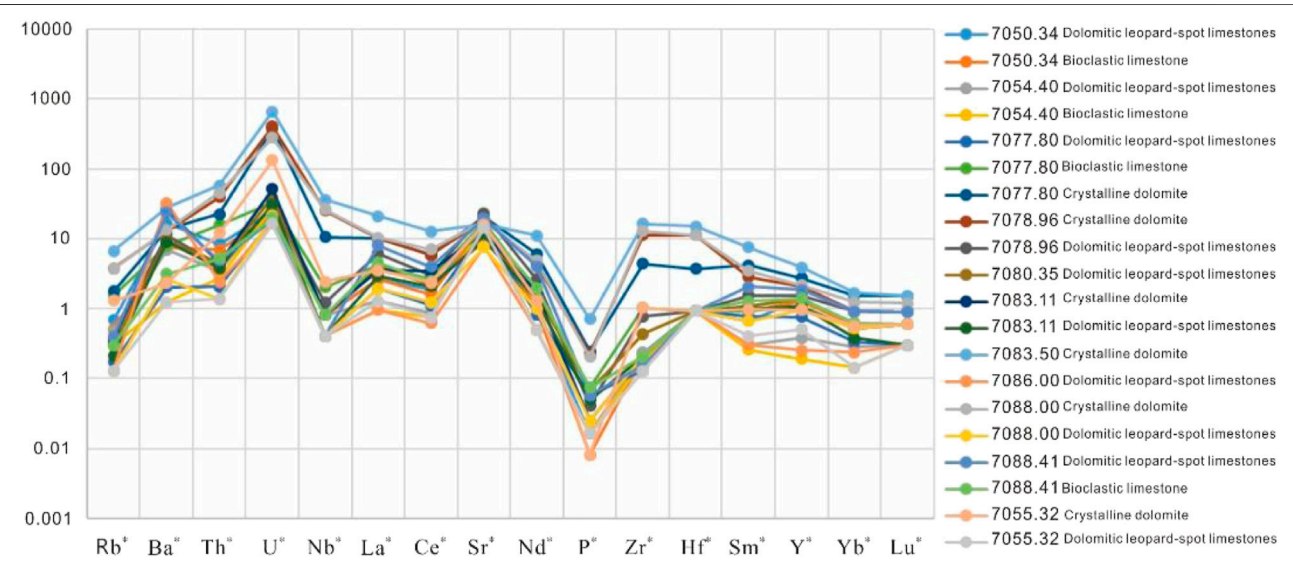

FIGURE 5 | Microelement distribution patterns in carbonate samples of Qixia Formation in the study area.

minerals (Lu, 2004). The homogeneous temperature can reflect the fluid temperature during the formation of minerals, thus permitting the extraction of valuable information during the mineral formation (Yue et al., 2005). According to statistics on 83 test points of dolomites in the study area, the uniform temperature of the dolomite inclusion of the Qixia Formation mainly ranges 68°C–135°C. A total of 42 inclusions were detected in the powder-fine crystalline dolomites in the dolomitic "leopard-spots," with a uniform temperature of 68°C–100°C. A total of 41 inclusions were tested from the crystalline dolomites, with a uniform temperature of 100°C–135°C. The uniform temperature of inclusions in the dolomitic "leopard-spots" and crystalline dolomite mainly ranges from 75°C to 110°C (**Figures 6A,B**). Furthermore, the uniform temperature of inclusions in pores and fillings at pore edges mainly ranges from 100°C to 130°C (**Figures 6C,D**).

6 DISCUSSIONS

6.1 Diagenetic Fluid Source and Formation of Dolomitic "Leopard-Spots"

6.1.1 C, O, and Sr Isotope Indexes

The atmospheric fresh water has a large variation range of $\delta^{13}C$, but its $\delta^{18}O$ is almost constant, and it usually possesses a high negative value. In the C and O isotopes of seawater, $\delta^{13}C$ and $\delta^{18}O$ skew to high positive values. In the buried environment, the

TABLE 3 | Order degree test data of dolomites of Qixia Formation in the study area.

Number of samples	Depth (m)	Lithology	Degree of order
QX10	7052.97	Dolomitic leopard-spot	0.49
QX20	7058.00	Crystalline dolomite	0.56
QX44	7083.50	Crystalline dolomite	0.68
QX47	7054.40	Dolomitic leopard-spot	0.4
QX55	7078.96	Crystalline dolomite	0.56
QX57	7083.11	Crystalline dolomite	0.51
QX58	7083.11	Crystalline dolomite	0.51
QX61	7086.00	Dolomitic leopard-spot	0.5
QX62	7088.00	Crystalline dolomite	0.5
QX63	7088.00	Crystalline dolomite	0.5
QX65	7088.41	Dolomitic leopard-spot	0.56
QX66	7088.41	Crystalline dolomite	0.53
QX67	7088.41	Dolomitic leopard-spot	0.48
QX68	7088.80	Crystalline dolomite	0.51

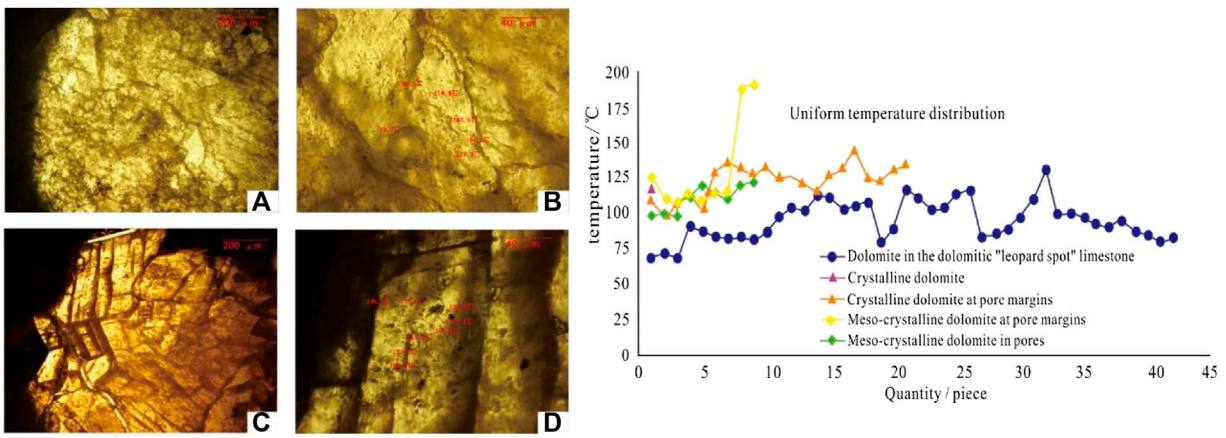

FIGURE 6 | Uniform temperature distribution of the fluid inclusion in dolomites of the Qixia Formation in the study area. **(A,B)** Inclusion test points in dolomitic "leopard-spots" and crystalline dolomites. **(C,D)** Inclusion test points in holes, pores, and seam edges.

$\delta^{18}O$ value skews toward the high negative value, and it is inversely proportional to the buried depth. We have to underline that the $\delta^{13}C$ value is relatively stable. Moreover, isotopes have different drift characteristics due to the influence of the different diagenesis environments (Wang et al., 2001; Wang et al., 2004; Zheng et al., 2008; Tian et al., 2014). The distribution of the C and O isotopes in dolomitic "leopard-spot" and base limestone are relatively similar in the Qixia Formation, showing the manifestation of general sea-source fluid environments similar to the diagenetic fluid of the limestone. The isotope of $\delta^{18}O$ of the dolomitic "leopard-spots" is apt to a negative high value, and the variation range of $\delta^{13}C$ is large. This reflects that the diagenetic fluid is dominated by contemporaneous seawater, interfering with the atmospheric fresh water. Moreover, diagenesis is influenced by high temperature to some extent.

Carbonate minerals mainly have three Sr sources: Earth's crust, mantle, and sea. As far as the Earth's crust source Sr is concerned, ^{87}Rb decays into radiogenic ^{87}Sr due to the long-term evolution, thus resulting in a high $^{87}Sr/^{86}Sr$ value (global average is 0.7119). The Earth's crust source Sr is mainly transferred by ancient rock weathering in lands and fresh water in rivers. The mantle source Sr refers to the relatively poor radiogenic Sr, which is provided by the hydrothermal system of the mid-oceanic ridge to seawater. Therefore, the ^{87}Sr content is relatively low (the global average is 0.7035). In this period, the mantle source Sr is provided by basalt eruption and invasion of Emei mantle movement. Interestingly, the sea source Sr is similar to the seawater and marine sediments at almost the same period. The variation range ($^{87}Sr/^{86}Sr$) of the Permian marine carbonate is 0.70662–0.70821 (Huang et al., 2002; McArthur and Howarth, 2005; Xie et al., 2022). The isotopes of $^{87}Sr/^{86}Sr$ of the dolomitic "leopard-spots" of the Qixia Formation in the study area are 0.70724–0.70934. It is slightly higher than those of the contemporaneous base limestones and seawater (Korte et al., 2005; Huang et al., 2011). Moreover, it is significantly higher than that of the Emei basalt. This effect indicates that the diagenetic fluid of dolomitization is similar to contemporaneous seawater,

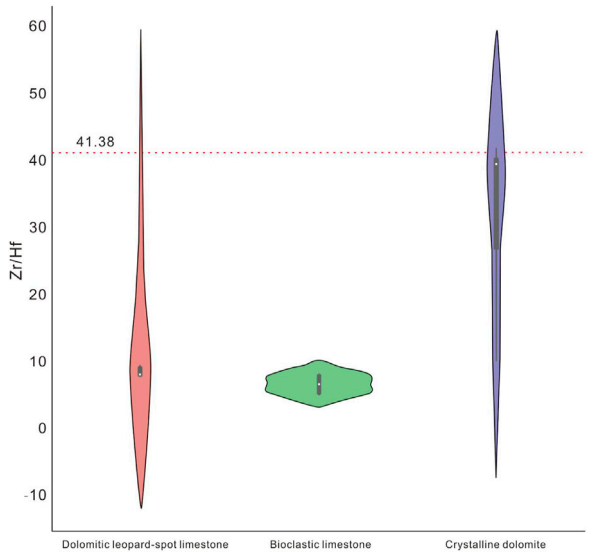

FIGURE 7 | Distribution of the Zr/Hf ratio of dolomite of Qixia Formation in the study area.

but it is not completely the same as the contemporaneous seawater fluid. Instead, the diagenetic fluid of dolomitization is influenced by some of Earth's crust source fluids, in which the upwelling fluid source containing mantle source Sr produced by underlying tectonic movement can be excluded.

6.1.2 Microelement Indexes

The content and distribution characteristics of microelements in rocks can reflect the elemental properties of diagenetic fluids when rocks were formed (Lottermoser, 1992; Webb and Kamber, 2000; Webb et al., 2009). Therefore, a deep discussion is often needed in the analysis of carbonate diagenetic fluid. The dolomitic "leopard-spots" of Qixia Formation in the study area have basically consistent characterization of the relatively stable elements (e.g., Na, K, Sr, and Ba) of marine water bodies with base limestones, showing similarity of their diagenetic fluids. Moreover, compared with the base limestones, the dolomitic "leopard-spots" have a higher Na, different K, and decreased Sr content, consistent with the characteristics of the crystalline dolomites. In other words, both the dolomitic "leopard-spots" and crystalline dolomites are influenced by similar exogenous fluids during the diagenetic process. Moreover, the distribution characterization of Rb, Ba, Th, U, Nb, La, Ce, Sr, Nd, P, Zr, Hf, Sm, Y, Yb, and Lu indicates that the diagenetic fluids of dolomitic "leopard-spots," base limestones, and crystalline dolomite are basically comparable.

From the elemental analysis, it can be argued that Zr and Hf are a pair of close concomitant elements (Huang et al., 2010). The provenance of rocks can be judged effectively by the ratio of Zr/Hf (**Figure 7**). Under this direction, the ratio of Zr/Hf has two obvious zones in samples. The part of the relatively low Zr/Hf value ranges between 5 and 8, averaging at 6.8. On the contrary, the part of the relatively high Zr/Hf value ranges between 30.1 and 44.7, averaging at 39.4. According to the upper crust standards (Zr = 240 μg/g, HF = 5.8 μg/g), the ratio of Zr/Hf is about 41.38. Hence, it can be speculated that terrigenous materials in the diagenetic fluids for dolomitic "leopard-spots" of the Qixia Formation might belong to the upper crust materials.

Based on the combination of the lithological and geochemical characteristics of the dolomitic "leopard-spots" of Qixia Formation in the study area, it can be speculated that this might be caused by the fast downward penetration of atmospheric fresh water and the flowing through seawater in the depositional stage. More specifically, it was formed in the contemporaneous ~ penecontemporaneous periods. The process of early dolomitization is controlled by the impact of the original sedimentary environment. Interestingly, fluids triggering dolomitization in different sedimentary environments are different to some extent (Machel, 2004). In the study area, the dolomites of the Qixia Formation were extensively developed and were significantly influenced by the landform high of Emei mantle uplift and atmospheric fresh water. The dolomitic "leopard-spots" developed in the seepage channel of the top seepage zone are involved with fresh water (**Figure 8**). Influenced by the sea surface, the atmospheric fresh water can provide long-term adjustment of the Ca^{+} and Mg^{+} balance in water bodies in the mixing belt of ancient landform highland and the underlying undercurrent belt. This effect is conducive to dolomitization at the top stratified sedimentation in the region within the reasonable geological term.

6.2 Dolomitization Fluid Temperature

The Sichuan Basin was strongly influenced by the Emei mantle plume movement during the Permian. In this period, the violent volcanic activities formed the Emeishan large igneous province, whereas magmatic eruption and magmatic intrusion were weakened gradually from south to north. Through a geologic age analysis of the basalt and relevant rocks in Emei Mountain, Fan (2004) pointed out that the basalt eruption in Emei Mountain was generally within 3 Ma from 253 to 256 Ma. Before the volcanic eruption, an uprising of the mantle column (wall) leads to the large-scale dome-shaped lifting effect. In addition, strong volcanic activities lead to corresponding heat flows in the Sichuan Province. According to the study of Zhu et al. (2010) on the paleo heat flow of several drillings in the Sichuan Basin, the paleo heat flow in the basin peaked at about 259 Ma, and a stage of sharp rising of paleo heat flow in the sedimentary stage (273–268 Ma) of Qixia Formation was recorded. This effect reflects that the formation temperature in the study area is far higher than that in normal sedimentation. Based on the O isotope equilibrium exchange principle between minerals and water, according to the literature, the dolomite-water O isotope fractionation equation under high and low temperatures can be obtained through experiments and calculations (Qian and Guo, 1998). Because dolomitization requires a relatively open environment, all previous formulas were developed using seawater as the experimental subject, whereas the fractionation coefficients in different regions at different periods were uncertain. According to the comparison of many calculation formulas of paleotemperature of several O isotopes and calibration by employing a uniform temperature of inclusion,

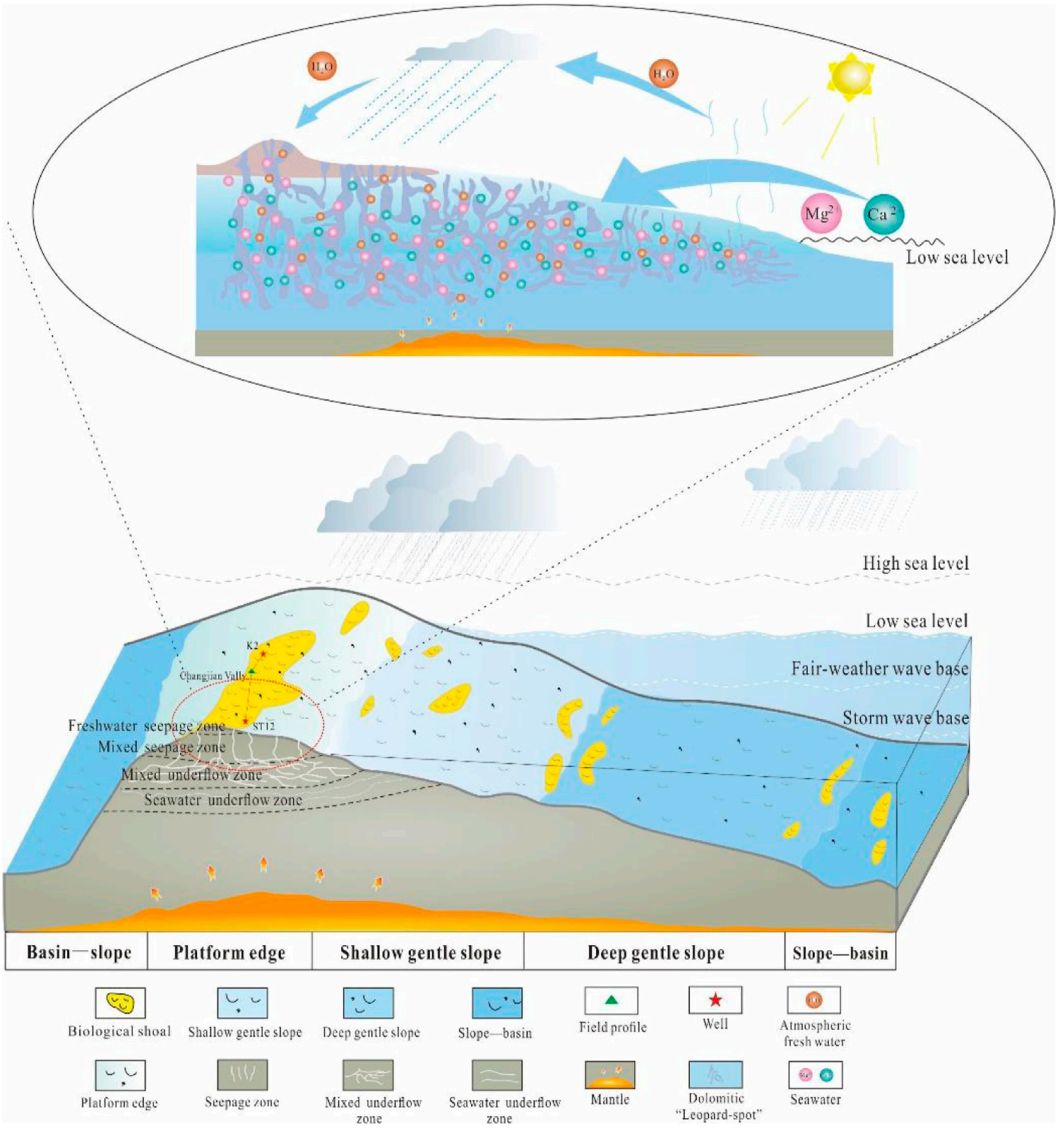

FIGURE 8 | Schematic diagram of diagenetic fluid migration and diagenetic model in the study area.

the calculation formulas of paleotemperature proposed by Land (1983) and Northrop and Clayton (1966) were chosen finally to calculate the diagenetic temperature of dolomite of the Qixia Formation in Shuangyushi Region on the northwestern Sichuan Basin. These two formulas have good applicability in calculating the diagenetic temperature of dolomites of the Qixia Formation in the study area:

$$10001\mathrm{na}_{(\mathrm{dolomite-water})} = 3.14 \times 10^{6}\mathrm{T}^{-2} - 2.0\,(\mathrm{Land}, 1983), \quad (1)$$

$$10001\mathrm{na}_{(\mathrm{dolomite-water})} = 3.20 \times 10^{6}\mathrm{T}^{-2} - 1.5\,(\mathrm{Narthrop}, 1966). \quad (2)$$

where 1000lna $_{(\mathrm{dolomite\text{-}water})}$ is the O isotope shunt coefficient between dolomite and water, which can be approximately expressed by $\delta^{18}O_{dolomite}$-$\delta^{18}O_{seawater}$. Besides, T stands for the Kelvin temperature.

This fractionation equation requires the existence of a relatively reasonable $\delta^{18}O$ value of contemporaneous seawater. In the study area, the ratio Sr/Mn of microelements reflects an extremely low alteration coefficient of the overall formation lithology. Consequently, the isotope of $\delta^{18}O$ (−1‰) of the bioclastic limestone in the dolomitic "leopard-spot" limestones was chosen for the calculation, and it was compared with the test temperature of inclusion. According to calculated results from **Eq. 1**, **Eq. 2**, the average diagenetic temperature of dolomites in the Qixia Formation was 67°C–73°C, with minimum and maximum values of 56.45°C and 80.66°C (**Table 4**). Moreover, the temperature climbed up gradually from up to the bottom (**Figure 9**), which proved the increasing paleo heat flow in the Chihsian Age in the study area.

In the test temperature, the lowest temperature exceeds the coarsening critical temperature (CRT > 50°C), indicating that the

TABLE 4 | Calculated results of the diagenetic temperature of dolomites of the Qixia Formation.

Number of samples	Depth (m)	$\delta^{18}O_{PDB}$	Land (1983)/°C	Northrop and Clayton (1966)/°C
QX3	7050.34	−2.97	56.45	62.32
QX10	7052.97	−3.45	59.21	65.18
QX47	7054.40	−3.12	57.00	62.89
QX14	7056.05	−3.94	62.04	68.11
QX18	7057.25	−4.91	67.92	74.21
QX20	7058.00	−5.1	69.14	75.47
QX24	7061.83	−5.49	71.61	78.04
QX25	7062.85	−5.30	70.37	76.75
QX30	7067.00	−5.30	70.37	76.75
QX53	7077.80	−4.33	64.36	70.51
QX55	7078.96	−5.35	69.37	76.75
QX42	7080.35	−5.11	69.14	75.47
QX57	7083.11	−4.67	66.13	72.35
QX44	7083.50	−5.88	74.14	80.66
QX59	7086.00	−4.91	67.92	74.21
QX62	7088.00	−5.25	69.75	76.11
QX65	7088.41	−4.85	67.32	73.59
QX68	7088.80	−4.71	66.72	72.97
QX46	7090.34	−5.59	72.24	78.69

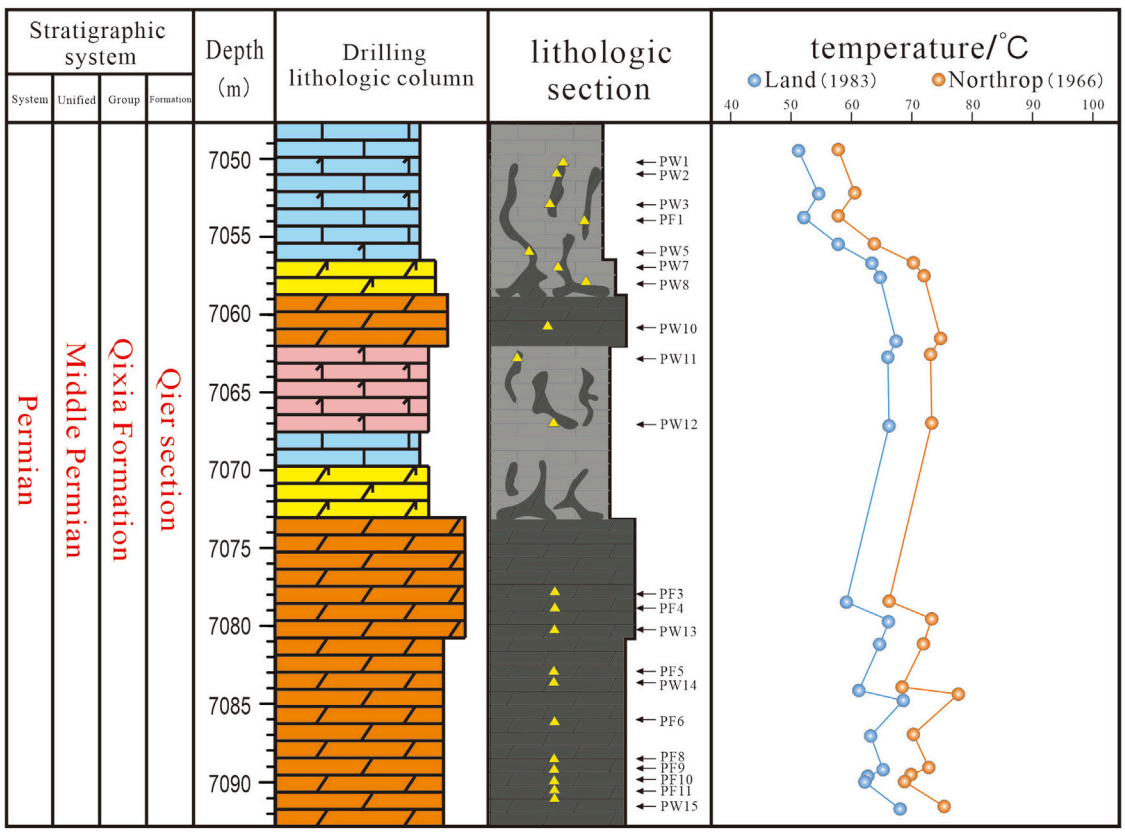

FIGURE 9 | Longitudinal distribution of the calculated diagenetic temperature of dolomites of Qixia Formation in Shuangyushi Region.

temperature conditions for the different crystal types or shallow buried high-temperature crystal variation characteristics have been reached (Gregg and Sibley, 1984; Sibley and Gregg, 1987; Machel, 2004) (**Figure 2I**). Combining with the order degree characteristics of dolomites, the fluid temperature of the general environment was relatively high in the Qixia Formation age. In

other words, the basic environmental temperatures for the formation of dolomitic "leopard-spots" and crystalline dolomite were relatively high (**Figure 8**).

6.3 Impact of "Leopard-Spot" Dolomites on Reservoir Accumulation

In the study area, the dolomitic "leopard-spots" were mainly composed of powder-fine crystalline dolomites, with relatively dense lithology and few visible pores. However, the dolomitic "leopard-spots" were partially filled with asphalt in local regions. The dolomitic "leopard-spots" can inherit rock pores better in the freshwater leaching karst system. Asphalt and macro-crystalline dolomites also filled in karst caves developed based on the dolomite plaques. Under the microscope, the relationship between the dolomitic "leopard-spot" and base limestones was relatively clear, which was formed after the irregular and uneven dolomitization reconstruction procedure of micritic-sparry bioclastic limestones. Sometimes, dolomite grains in dolomitic "leopard-spots" were found in regular euhedral shape (**Figures 2F,G**) or anhedral-subhedral mosaic shape, with local residues of non-metasomatic creatures (**Figures 2F–H**). However, intergranular holes and intergranular pores were poorly developed, with a general porosity of 1%–2%. Moreover, these intergranular holes and intergranular pores were mainly filled with plaster, clay mud, and organics. The accumulation is generally manifested by relatively poor "saccharoidal" dolomites at the bottom of the relative formations. However, the dolomitic "leopard-spots" can be used as the seepage channel of the diagenetic fluid. More specifically, they not only changed the diagenetic fluid characteristics of the underlying thick-layered crystalline dolomite but also were conducive to the development of reservoir construction such as karst and were of vital significance for exploring dolomite reservoirs of the Qixia Formation in the study area (Machel, 2004; Zheng et al., 2008; Chen et al., 2013; Zheng and Qin, 2020).

7 CONCLUSION

1) The dolomites of the Middle Permian Qixia Formation in Shuangyushi Region in northwestern Sichuan Basin mainly include two types of dolomitic: "leopard-spot" limestones and crystalline dolomite. Moreover, the dolomitic "leopard-spot" limestones were often above crystalline dolomites. The dolomitic "leopard-spots" were found in the vertical distribution and changed to thick-layered massive crystalline dolomites gradually. The longitudinal distributions of the dolomitic "leopard-spot" limestones and crystalline dolomite exhibited some cycles and were controlled by the sedimentary environment. The dolomitic "leopard-spots" were developed with pores, which accumulate reservoirs to some extent.
2) In the dolomitic "leopard-spot" limestones of the Qixia Formation, dolomitic "leopard-spot" and base limestones exhibited basically similar geochemical properties and consistent diagenetic period. Both were formed in the contemporaneous-penecontemporaneous periods. The diagenetic fluids were contemporaneous seawater and involved atmospheric fresh water. However, some distinct differences in geochemical characteristics between dolomitic "leopard-spots" and crystalline dolomites were observed. This outcome reveals that crystalline dolomites suffered from the stronger intervention of exogenous freshwater fluids and were subjected to burial dolomitization and hot-press dolomitization processes in the late stage.
3) For the Middle Permian Qixia Formation in the Shuangyushi Region in northwestern Sichuan Basin, the dolomitic "leopard-spot" limestones and the underlying crystalline dolomite formed the diagenetic fluid, which has characteristics of up-down seepage in the open water bodies and relatively high paleogeotemperature background. Neither excessive dolomite growth nor hydrothermal dolomitization was caused by multi-age, and the long-term reflux penetration mode proposed by predecessors can interpret the formation of dolomitic "leopard-spots" and powder-fine crystalline dolomites in Qixia Formation completely. In the study area, the dolomite genesis process could be attributed to dolomitization involving fresh water in the high-temperature environment from the contemporaneous period to the early burial stage.

DATA AVAILABILITY STATEMENT

The original contributions presented in the study are included in the article/Supplementary Material. Further inquiries can be directed to the corresponding authors.

AUTHOR CONTRIBUTIONS

SX: data curation and writing original draft; XW, BL, and HJ: project administration and supervision; YD, RZ, YL, MW, DH, and JK: resources and investigation; FH and BZ: reviewing and editing.

FUNDING

This research was supported by the China National Science and Technology Major Project (2016ZX05007004-001, 2017ZX05001001-002), Petro-China Innovation Foundation (2018D-5007-0105), Scientific Research Starting Project of SWPU (2017QHZ005).

ACKNOWLEDGMENTS

The authors thank experts for constructive suggestions; Lin Xie of the Southwest Petroleum University for their guidance and help in using the instrumentations; and Master Yawen Li, Yangyang Zhang, and Mingyang Ma of the Southwest Petroleum University for data collation and part of the drawing.

REFERENCES

Badiozamani, K. (1973). The Dorag Dolomitization Model,application to the Middle Ordovician of Wisconsin[J]. *J. ofSedimentary Res.* 43 (4), 965–984. doi:10.1306/74d728c9-2b21-11d7-8648000102c1865d

Bathurst, R. G. C. (1975). *Carbonate Sediments and Their Diagenesis*(Second Edition)[J].New York:Elsevier, Vol.1-658.

Bo, L., Wang, X., Xie, S., Feng, M., Yang, X., Huo, F., et al. (2020). Characteristics and Genesis of the Middle Permian Qixia Formation Dolomite in the Northwestern Sichuan Basin[J]. *Chin. J. Geol. Geol. Sinica* 55, 183–199. doi:10.12017/dzkx.2020.013

Boynton, W. V. (1984). *Cosmochemistry of the Rare Earth Elements; Meteorite Studies[M]*. Amsterdam: Elsevier Science Publishing Company.

Budd, M. A. (1997). Introduction. *Earth-Science Rev.* 42 (1-2), 1–10. doi:10.1057/9780230377127_1

Chen, X., Zhao, W., Liu, Y., Zhou, H., and Jiang, Q. (2013). Characteristics and Exploration Strategy of the Middle Permian Hydrothermal Dolomite in Southwestern Sichuan Basin[J]. *Acta Pet. Sin.* 34 (3), 460–466. doi:10.7623/syxb201303006

Fan, W. (2004). Ar-Ar and U-Pb Geochronology of Late Paleozoic Basalts in Western Guangxi and Their Constraints on the Eruption Age of Emeishan Basalt Province[J]. *Chin. Sci. Bull.* 18, 1892–1900. doi:10.1360/04wd0201

Friedman, G. M. (1980). Dolomite Is an Evaporite Mineral: Evidence from the Rock Record and from Sea-Marginal Ponds of the Red Sea. *Concepts Models Dolomitization* 28, 69–80. doi:10.2110/pec.80.28.0069

Gregg, J. M., and Sibley, D. F. (1984). Epigenetic Dolomitization and the Origin of Xenotopic Dolomite Texture. *J. Sediment. Petrology* 54 (3), 908–931. doi:10.1306/212f8535-2b24-11d7-8648000102c1865d

Guo, F., Peng, H., Pan, J., Du, Y., Liu, L., Luo, N., et al. (2003). A Probe into the Carbon and Oxygen Isotopic Characteristics of the Cambrian Carbonate Rocks in Jiangshan, Zhejiang and its Paleo-Environment Significance[J]. *J. Stratigr.* 4, 289–297. doi:10.1016/S0955-2219(02)00073-0

Guoqi, W., Yang, W., Zhu, Y., Jin, H., Li, Y., Shi, Z., et al. (2010). Depositional System of the Middle Permian Qixia Formation in the Western Sichuan Basin [J]. *Oil Gas Geol.* 31 (4), 442–448. doi:10.11743/ogg20100407

Han, X., Bao, Z., and Xie, S. (2016). Origin and Geochemical Characteristics of Dolomites in the Middle Permian Formation, SW Sichuan Basin, China[J]. *Earth Sci.* 41 (1), 167–176. doi:10.3799/dqkx.2016.013

He, Y., and Feng, Z. (1996). Origin of Fine-to Coarse-Grained Dolostones of Lower Permian in Sichuan Basin and its Peripheral Regions[J]. *J. Oil Gas Technol.* 18 (4), 15–20.

Hu, M., Guoqi, W., and Hu, Z. (2010). Sequence-lithofacies Palaeogeography of the Middle Permian Qixia Formation in Sichuan Basin[J]. *J. Palaeogeogr.* 12 (5), 515–526. doi:10.1017/S0004972710001772

Hu, D., Wang, L., Huang, R., Duang, J., Xu, Z., and Pan, L. (2019). Characteristics and Main Controlling Factors of the Middle Permian Maokou Dolomite Reservoirs in the Eastern Sichuan Basin[J]. *Nat. Gas. Ind.* 39 (6), 13–21.

Huang, S., Shi, H., Zhang, M., Shen, L., and Wu, w. (2002). Application of Strontium Isotope Stratigraphy to Diagenesis Research[J]. *Acta Sedimentol. Sin.* 20 (3), 359–366. doi:10.1007/s11769-002-0045-5

Huang, S. (2010). *Carbonate Diagenesis[M]*. Beijing: Geological Publishing, 56–57.

Huang, S., Huang, Y., Lan, Y., and Huang, K. K. (2011). A Comparative Study on Strontium Isotope Composition of Dolomites and Their Coeval Seawater in the Late Permian-Early Triassic[J]. *Acta Petrol. Sin.* 27 (12), 3831–3842. doi:10.1016/S1002-0160(11)60127-6

Huang, S., Li, X., Huang, K., Lan, Y., and Lv, J. (2012). Authigenic Noncarbonate Minerals in Hydrothermal Dolomite of Middle Permian Qixia Formation in the West of Sichuan Basin, China[J]. *J. Of Chengdu Univ. Of Technol. Sci. Technol. Ed.* 39 (4), 343–352. doi:10.1177/1687814015604547

Huang, S., Lan, Y., Huang, K., and Lv, J. (2014). Vug Fillings and Records of Hydrothermal Activity in the Middle Permian Qixia Formation, Western Sichuan Basin[J]. *Acta Petrol. Sin.* 30 (3), 687–698. doi:10.1134/S1075701514020044

Jiang, Z., Wang, X., Zeng, D., Lu, T-M., Wang, B-Q., and Zhang, J-Y. (2009). Constructive Diagenesis and Porosity Evolution in the Lower Permian Qixia Formation of Northwest Sichuan[J]. *Geol. China* 36 (1), 101–109. doi:10.1016/S1874-8651(10)60080-4

Korte, C., Jasper, T., Kozur, H. W., and Veizer, J. (2005). δ18O and δ13C of Permian Brachiopods: A Record of Seawater Evolution and Continental Glaciation. *Palaeogeogr. Palaeoclimatol. Palaeoecol.* 224, 333–351. doi:10.1016/j.palaeo.2005.03.015

Land, L. S. (1983). "The Application of Stable Isotopes to Studies of the Origin of Dolomite and to Problems of Diagenesis of Clastic Sediments," in *Stable Isotopes in Sedimentary Geology, SEPM Short Course 10*. M. A. Arthur and T. F. Anderson (Tulsa: Society for Senimentary Geology), 1–22.

Li, M., Tan, X., Luo, B., Zhang, Y., Zhang, B., Lu, F., et al. (2020). Characteristics of Facies-Controlled and Early High-Frequency Exposed Karstificationin the Qixia Formation of Middle Permian in the Northwest of Sichuan Basin and its Significance[J]. *China Pet. Explor.* 25 (3), 55–70.

Longman, M. W. (1980). Carbonate Diagenetic Textures from Near Surface Diagenetic Environments[J]. *AAPG Bull.* 64 (4), 461–487. doi:10.1306/2f918a63-16ce-11d7-8645000102c1865d

Lottermoser, B. G. (1992). Rare Earth Elements and Hydrothermal Ore Formation Processes. *Ore Geol. Rev.* 7, 25–41. doi:10.1016/0169-1368(92)90017-f

Lu, H. (2004). *Fluid Inclusion[M]*. Beijing: Science Press.

Lu, F., Tan, X., Zhong, Y., Luo, B., Zhang, B., Zhang, Y., et al. (2020). Origin of the Penecontemporaneous Sucrosic Dolomite in the Permian Qixia Formation,northwestern Sichuan Basin,SW China[J]. *Petroleum Explor. Dev.* 47 (06), 1134–1148+1173. doi:10.1016/s1876-3804(20)60131-3

Luo, L., Wang, X., Li, Y., Zhang, R., and Wang, N. (2017). Sedimentary Facies in Middle Permian Series in Northwest Sichuan and its Effect on Reservoirs[J]. *Special Oil Gas Reservoirs* 24 (4), 60–66. doi:10.3969/j.issn.1006-6535.2017.04.011

Machel, H.-G., and Mountjoy, E. W. (1986). Chemistry and Environments of Dolomitization -A Reappraisal. *Earth-Science Rev.* 23 (3), 175–222. doi:10.1016/0012-8252(86)90017-6

Machel, H. G. (2004). Concepts and Models of Dolomitization: A Critical Reappraisal. *Geol. Soc. Lond. Spec. Publ.* 235 (1), 7–63. doi:10.1144/gsl.sp.2004.235.01.02

Mazzullo, S. J. (2009). Organogenic Dolomitization in Peritidal to Deep-Sea Sediments[J]. *J. Sediment. Res.* 70 (1), 10–23. doi:10.1306/2dc408f9-0e47-11d7-8643000102c1865d

McArthur, J. M., and Howarth, R. J. (2005). "Strontium Isotope Stratigraphy," in *A Geologic Time Scale 2004[M]*. Editors F. Gradstein, J. Ogg, and A. Smith (Cambridge: Cambridge University Press), 96–105. doi:10.1017/cbo9780511536045.008

Northrop, D. A., and Clayton, R. N. (1966). Oxygen Isotope Fractionations in Systems Containing Dolomite. *J. Geol.* 74 (2), 174–196. doi:10.2307/30065685

Qian, Y., and Guo, J. (1998). Experimental Study of Hydrogen Isotope Equilibrium and Kinrtic Fractionation for the Mineral Water Systems[J]. *Geosci. Front.* 2, 251–261. doi:10.1088/0256-307X/16/9/027

Sibley, D. F., and Gregg, J. M. (1987). Classification of Dolomite Rock Texture. *J. Sediment. Res.* 57 (6), 967–975. doi:10.1306/212F8CBA-2B24-11D7-8648000102C1865D

Sibley, D. F. (1991). Secular Changes in the Amount and Texture of Dolomite. *Geol* 19, 151–154. doi:10.1130/0091-7613(1991)019<0151:scitaa>2.3.co;2

Song, W. (1985). Distribution and Natural Gas Exploration of Permian Dolomite in Sichuan Basin[J]. *Nat. Gas. Ind.* 5 (4), 16–23.

Tian, J., Lin, X., Zhang, X., Peng, S., Yang, C., Luo, S., et al. (2014). The Genetic Mechanism of Shoal Facies Dolomite and its Additive Effect of Permian Qixia Formation in Sichuan Basin[J]. *Acta Petrol. Sin.* 30 (3), 679–686.

Tucker, M. E. (1991). *Carbonate Sedimentology[M]*. Incorporated: Wiley-Blackwell [Imprint];John Wiley & Sons.

Vasconcelos, C., Mckenzie, J. A., Bernasconi, S., Grujic, D., and Tiens, A. J. (1995). Microbial Mediation as a Possible Mechanism for Natural Dolomite Formation at Low Temperatures. *Nature* 377 (6546), 220–222. doi:10.1038/377220a0

Wang, D., and Bai, Y. (1999). An Expression of Palaeoclimate by Stable Isotopes in Carbonate Sedimentary[J]. *Petroleum Explor. Dev.* 6 (5), 30–32. doi:10.1006/mcpr.1998.0211

Wang, Q., Shi, J., Chen, G., Chen, G., and Xue, L. (2001). Characteristics of Diagenetic Environments of Carbonate Rocks in Western Tarim Basin and Their Controls on the Reservoir Property[J]. *Acta Sedimentol. Sin.* 19 (4), 548–556. doi:10.3969/j.issn.1000-0550.2001.04.012

Wang, F., Chen, Z., Wang, X., and Tian, J. (2004). Diagenesis and Reservoir Characterization Carboniferous Sediments in Northeastern Sichuan[J]. *Mar. Orig. Pet. Geol.* 1, 91–96. doi:10.3969/j.issn.1672-9854.2004.01.010

Wang, K., Li, W., Jin, L., and Zhang, C. (2011). Carbon Oxygen, Strontium Isotope Characteristics and Cause Analysis of Carboniferous Carbonate Rocks in the Eastern Sichuan Basin[J]. *J. Earth Sci.* 40 (4), 351–362. doi:10.1007/s11589-011-0776-4

Wang, N., Wei, G., Yang, W., and Wang, Y. (2016). Formation and Evolution of Jiange Paleo-Uplift in Northwestern Sichuan Basin and Gas-Controlled Effect [J]. *Xinjiang Pet. Geol.* 37 (2), 125–130. doi:10.7657/XJPG20160201

Warren, J. (2000). Dolomite: Occurrence, Evolution and Economically Important Associations[J]. *Earth Sci. Rev.* 52 (1), 1–81. doi:10.1016/s0012-8252(00)00022-2

Webb, G. E., and Kamber, B. S. (2000). Rare Earth Elements in Holocene Reefal Microbialites: a New Shallow Seawater Proxy. *Geochimica Cosmochimica Acta* 64, 1557–1565. doi:10.1016/s0016-7037(99)00400-7

Webb, G. E., Nothdurft, L. D., Kamber, B. S., Kloprogge, J. T., and Zhao, J.-X. (2009). Rare Earth Element Geochemistry of Scleractinian Coral Skeleton during Meteoric Diagenesis: a Sequence through Neomorphism of Aragonite to Calcite. *Sedimentology* 56, 1433–1463. doi:10.1111/j.1365-3091.2008.01041.x

Xie, S., Wang, X., Li, B., Wen, L., Xu, L., Du, Y., et al. (2022). The Behavior of REEs Indicates the Dolomite Petrogenesis and a Unique Dolomitization Model of the Middle Permian Qixia Formation in Northwest Sichuan Basin, China[J]. *Carbonates and Evaporites* 37 (2). doi:10.1007/s13146-022-00765-6

Xu, J., Xiao, D., Su, W., Yan, W., Zhong, S., Yang, M., et al. (2022). Characteristics and Genesis of Leopard Porphyry Dolomitic Limestone in the Fourth Member of Ordovician Majiagou Formation in the Eastern Margin of Ordos Basin: Taking Guanjiaya Section as an Example[J]. *J. Palaeogeogr.* 24 (2), 261–277.

Yan, Z., Guo, F., Pan, J., Guo, G., and Zhang, R. (2005). Application Of C, O and Sr Isotope Composition of Carbonates in the Research of Paleoclimate and Paleooceanic Environment. *Contrib. Geol. Miner. Resour. Res.* 20 (1), 53–56,65. doi:10.3969/j.issn.1001-1412.2005.01.010

Yang, W., Zhang, T., Liu, Z., Huang, H., Min, H., and Yang, Y. (2014). Sedimentary and Environmental Responses to Mantle Plume: A Case Study of Emeishan Mantle Plume[J]. *Acta Petrol. Sin.* 30 (3), 835–850. doi:10.1093/ps/79.11.1669

Yuan, Q., Li, B., Liu, H., Liu, S., and Wang, L. (2010). The Tectonics Evolution and Lithofacies Palaeogeography in the Northwest of the Sichuan Basin[J]. *J. Daqing Petroleum Inst.* 6, 42–52. doi:10.3969/j.issn.2095-4107.2010.06.008

Yue, L., Zhou, Y., and Yan, S. (2005). Application of Fluid Inclusion in Hydrocarbon Exploration[J]. *J. Oil Gas Technol.* 6 (205), 711–714.

Zhang, T., Chen, X., Liu, Z., Wei, G., Yang, W., Min, H., et al. (2011). Effect of Emeishan Mantle Plume over the Sedimentary Pattern of Mid-permian Xixia Period in Sichuan Basin[J]. *Acta Geol. Sin.* 85 (8), 1251–1264. doi:10.1007/s12182-011-0118-0

Zhang, Y. (1982). Dolomitization in Permian in Sichuan Basin[J]. *Acta Pet. Sin.* 3 (1), 29–33. doi:10.7623/syxb198201005

Zhao, W., Shen, A., Qiao, Z., Pan, L., Hu, A., and Zhang, J. (2018). Genetic Types and Distinguished Characteristics of Dolomite and the Origin of Dolomite Reservoirs[J]. *Petroleum Explor. Dev.* 45 (6), 923–935. doi:10.11698/PED.2018.06.01

Zheng, R., Hu, Z., Chao, Z., Chen, S., and Dai, L. (2008). Geochemical Characteristics of Stable Isotopes in Paleokarst Reservoirs in Huanglong Formation in Northern Chongqing-Eastern Sichuan Area[J]. *Earth Sci. Front.* 15 (6), 303–311.

Zheng, Z., and Qin, W. (2020). Research Progress on Ordering and Rheological Properties of Dolomite[J]. *Geol. J. China Univ.* 26 (2), 197–208.

Zhu, C., Tian, Y., Xu, M., Rao, S., Yuan, Y., Zhao, Y., et al. (2010). The Effect of Emeishan Supper Mantle Plume to the Thermal Evolution of Source Rocks in the Sichuan Basin[J]. *Chin. J. Of Geophys.* 53 (1), 119–127. doi:10.1002/cjg2.1475

Conflict of Interest: BL was employed by the Shale Gas Research Institute of PetroChina Southwest Oil & Gasfield Company. HJ, RZ, YL, and BZ were employed by the Exploration Division of PetroChina Southwest Oil & Gasfield Company. YD was employed by PetroChina Southwest Oil & Gasfield Company.

The remaining authors declare that the research was conducted in the absence of any commercial or financial relationships that could be construed as a potential conflict of interest.